

Human–Robot Interaction via the Transfer of Power and Information Signals

H. KAZEROONI, MEMBER, IEEE

Abstract—A human's ability to perform physical tasks is limited not by intelligence, but by physical strength. If, in an appropriate environment, a machine's mechanical power is closely integrated with a human arm's mechanical power under the control of the human intellect, the resulting system will be superior to a loosely integrated combination of a human and a fully automated robot. Therefore, a fundamental solution to the problem of "extending" human mechanical power must be developed. The work presented defines "extenders" as a class of robot manipulators worn by humans to increase human mechanical strength while the wearer's intellect remains the central control system for manipulating the extender. The human, in physical contact with the extender, exchanges power and information signals with the extender. This analysis focuses on the dynamics and control of human–robot interaction in the sense of the transfer of power and information signals. General models for the human, the extender, and the interaction between the human and the extender are developed. The stability of the system of human, extender, and the object being manipulated is analyzed and the conditions for stable maneuvers are derived. An expression for the extender performance is defined to quantify the force augmentation. The trade-off between stability and performance is described. The theoretical predictions are verified experimentally.

I. INTRODUCTION

THE ability of a robot manipulator to perform a task depends upon the available actuator torque: a relatively small hydraulic actuator can supply a large torque. In contrast, the muscular strength of the average human is quite limited. Extenders are defined as a class of robot manipulators which extend the strength of the human arm while maintaining human control of the task. The defining characteristic of an extender is the "transmission of power and information signals." The extender is worn by the human; the physical contact between the extender and the human allows direct transfer of mechanical power and information signals.¹ Because of this unique interface, control of the extender trajectory can be accomplished without any type of joystick, keyboard, or master–slave system. The human provides a control system for the extender, while the extender actuators provide most of the strength

necessary for the task. The human becomes a part of the extender and "feels" a scaled-down version of the load that the extender is carrying. The extender is distinguished from a conventional master–slave² system. In contrast, in a conventional master–slave system, the human operator is either at a remote location or close to the slave manipulator, but is not in direct physical contact with the slave in the sense of transfer of power. Thus the operator can exchange information signals with the slave, but cannot directly exchange mechanical power. A separate set of actuators is required on the master to reflect forces³ felt by the slave back to the human operator.⁴

The input to the extender is derived from the contact forces between the extender and the human. The contact force is measured, appropriately modified (in the sense of control theory to satisfy performance and stability criteria), and used as an input to the extender control, in addition to being used for actual maneuvering. Because force reflection occurs naturally in the extender, the human arm feels a scaled-down version of the actual forces on the extender *without* a separate set of actuators. For example, if an extender is employed to manipulate a 100-lbf object, the human may feel 10 lbf while the extender carries the rest of the load. The 10-lbf contact force is used not only to manipulate the object, but also to generate the appropriate signals to the extender controller.

Fig. 4(a), which is used to describe several concepts, shows a simple one-degree-of-freedom extender imposing large forces on the environment. This experimental extender consists of an outer tube and an inner tube. The human arm, wrapped in a cylinder of rubber for a snug fit, is located in the inner tube. A piezoelectric load cell, placed between these tubes, measures the interaction force between the human arm and the extender. A rotary hydraulic actuator, mounted on a platform, powers the extender. Fig. 1 shows the author's conception of the archi-

Manuscript received January 6, 1989; revised August 27, 1989.

The author is with the Mechanical Engineering Department, University of Minnesota, 111 Church Street SE, Minneapolis, MN 55455.

IEEE Log Number 8933035.

¹Human–machine interaction in active systems has been traditionally characterized by the exchange of "information signals" only. For example, in human–computer interaction, the human sends information signals to the computer via a keyboard. In another example, a person sends an information signal to an electric mixer by pushing buttons. There is no power transfer between the person and the mixer motor; the person does not feel the load on the mixer motor.

²A master–slave system (teleoperator system) uses a control joystick of a geometry similar to that of the slave manipulator for input. The joystick (master) has position transducers at the joints to measure displacement, and the output from these transducers is used as an input to the manipulator (slave). Thus, the motion of the manipulator follows that of the joystick. Ideally, the motion of the slave will be identical to that of the master.

³In this paper, "force" implies force and torques, and "position" implies position and orientation.

⁴The elimination of force feedback in remote master–slave manipulation may result in poor positioning precision and possible instability.

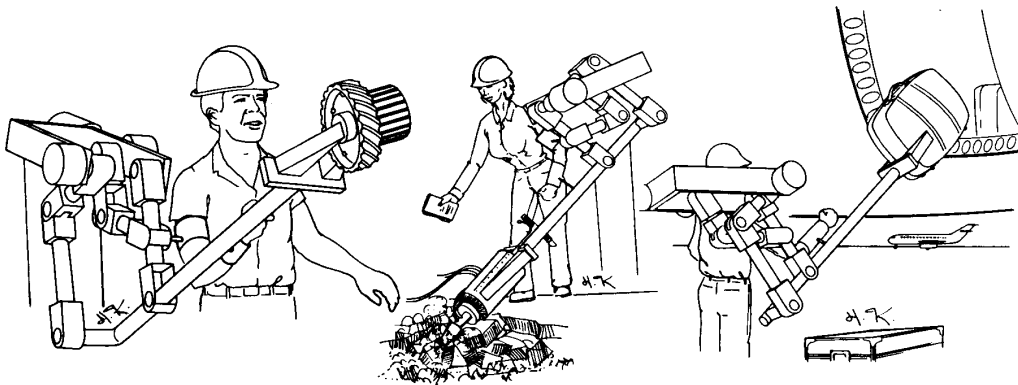


Fig. 1. Author's conception of multidegree-of-freedom extender being built at University of Minnesota.

ture for a prototype multidegree-of-freedom extender being built at the University of Minnesota. For clarity, the sleeve into which the human's arm would be inserted is not shown and the extender is shown without a base. In reality, the extender might be attached to a mobile or stationary base.

This article establishes a set of experimentally verified ground rules for control of human-machine interaction in the sense of transfer of power and information signals. Section II is devoted to the history and background relevant to this work. Sections III-VI describe the dynamic behavior of the extender and human, and their interaction. Section VII gives a mathematical description of extender performance. Sections VIII and IX derive the stability condition for the system of extender, human, and object being manipulated. The expressions for performance and for the stability condition reveal the trade-offs between the degree of performance and the stability range. This leads to Sections X-XIII, which give a detailed theoretical and experimental description of the stability and performance of a prototype extender.

II. HISTORY AND BACKGROUND

The concept of a device to increase the strength of a human operator using a master-slave system has existed since the early 1960's and was originally named "man-amplifier." The man-amplifier was defined as a manipulator which would greatly increase the strength of a human operator while maintaining human control of the manipulator. Note that these early systems were based upon the master-slave concept rather than upon direct physical contact between human and manipulator.

In the early 1960's, the Department of Defense was interested in developing a powered "suit of armor" to augment the lifting and carrying capabilities of soldiers. The original intent was to develop a system which would allow the human operator to walk and to manipulate very heavy objects. In 1962, research was done for the Air Force at the Cornell Aeronautical Laboratory to determine the feasibility of developing a master-slave system to accomplish this task [2]. This study determined that dupli-

cating all human motions would not be practical, and that further experimentation would be required to determine which motions were necessary. It was also determined that the most difficult problems in designing the man-amplifier were in the areas of servo, sensor, and mechanical design.

The Cornell Aeronautical Laboratory did further work on the man-amplifier concept [16] and determined that an exoskeleton (an external structure in the shape of the human body), having far fewer degrees of freedom than the human operator, would be sufficient for most desired tasks. A preliminary arm and shoulder design, developed at Cornell in 1964, determined that the physical size of the hydraulic actuators limited the manipulator's amplifying ability.

Further work on the human-amplifier concept, through prototype development and testing, was carried out at General Electric from 1966 to 1971 [4]-[6], [14], [17], [18]. This man-amplifier, known as the Hardiman, was designed as a master-slave system. The Hardiman was a set of overlapping exoskeletons worn by the human operator. The master portion was the inner exoskeleton, which followed all the motions of the operator. The outer exoskeleton consisted of a hydraulically actuated slave, which followed all the motions of the master. Thus the slave exoskeleton also followed the motions of the operator.

In contrast with the Hardiman and other man-amplifiers, the extender is not a master-slave system. Instead, the human operator's commands to the extender are taken directly from the interaction force between the human and the extender. This interaction force also helps the extender manipulate an object. The extender controller translates the signals representing the interaction force into a motion command for the extender. Thus the human initiates tracking commands to the extender in a natural way.⁵ The controller also regulates the interaction force to be a

⁵A point must be made about what we mean by "natural way." If "talking" is defined as a natural method of communication between two people, then we would like to communicate with a computer by talking rather than by using a keyboard. The same is true here: if we define "maneuvering the hands" as a natural method of moving loads, then we would like to move only our hands to maneuver a load, rather than by using a keyboard or joystick.

desired force reflection on the human. The human operator *can feel* the scaled-down effect of loads and/or interaction forces on the extender because the forces acting on the extender are reflected back naturally.

Some major areas of application for the extender include manufacturing, construction, loading and unloading aircraft, maneuvering cargo in shipyards, foundries, mining, or any situation which requires precise and complex movement of heavy objects. In contrast with existing systems, such as forklifts, pulleys, and cranes, the extender lets the human adjust the orientation of objects. Due to the natural communication between the human and the extender, the extender has major advantages over conventional methods of manipulating heavy objects.

- 1) The human needs very *little training* to operate the extender in contrast with driving a system via keyboards and joysticks.
- 2) The human can *react quickly* to provide an input to the extender because the forces acting on the extender are fed back naturally. For example, the operator can orient a heavy object faster with an extender.
- 3) The human operator *can feel* the scaled-down effect of loads and/or interaction forces on the extender because the forces acting on the extender are reflected back. A master-slave system needs two sets of actuators for force reflection on the human.
- 4) The operator can maneuver heavy objects much more *naturally*. For example, if an object is falling, the operator can prevent the fall more quickly.

The extender also can serve as an upper limb orthosis, enhancing existing motor ability in the physically impaired. An orthosis is an externally applied device which improves the functionality of an impaired limb⁶ in contrast with a prosthesis, which replaces body segments [1], [19]. The extender orthosis would augment the lifting ability of the patient and also allow continued use of the patient's remaining motor ability. To employ the extender, the patient must have some ability to move his arm and thus drive the extender. The extender would serve to improve the patient's limb function while utilizing the remaining natural limb function. Instead of promoting muscle atrophy, the extender system could be therapeutic and promote further muscle development in the limb.

The first tests on a motor-controlled upper limb orthosis were carried out in 1956 [1]. This was a myoelectric⁷ system, which used the electrical output of contracting muscles as a control input. Striated muscles drive body segments and are composed of many motor units. When a

striated motor unit is contracted, an electrical signal is generated by the depolarization, which initiates the contraction. The sum of the depolarizations from all motor units in the muscle is known as an electromyographic or EMG signal. One disadvantage of using EMG signals is cross talk from other contracting muscles in the region of interest, which may interfere with the desired input. In addition, the signal obtained from the muscles is very small, and thus, noise may be a serious problem. Also, considerable concentration is required to perform manipulation with more than one degree of freedom; this has a serious effect on patient acceptance of the device.

A second alternative for command generation is the mechanical input system. Mechanical input systems rely on a joystick or other input device to initiate a control command. The orthosis follows the motion of the joystick: up-down, left-right, or backward-forward. A disadvantage of this system is the coupling of the joystick motion with the orthosis motion. A third alternative for command generation is the photoelectric system, which converts light energy to electric energy for use as a command signal. Such a system requires a light source which can be manipulated by the patient and photocells to convert energy [3].

III. DYNAMIC BEHAVIOR OF THE EXTENDER

Considering the extender as a mechanism composed of rigid members, the dynamic behavior of an open-loop extender (without any control feedback) can be derived by a set of nonlinear differential equations via the Lagrangian [7] or Eulerian approaches. However, the rigid body dynamics are not sufficient for modeling if there are other significant dynamic components in the system. For example, if hydraulic actuators are chosen to power the extender, then the dynamic behavior of the actuators may be a considerable factor which must be integrated into the total dynamic behavior of the extender. Transmission systems, when used to drive the extender, may also contribute to the extender dynamics. Therefore, the objective here is to develop an unstructured dynamic model [10] that can represent the complete dynamic behavior of the extender in a very general form. This unstructured model focuses on the relationship between the input and output properties of the extender, and thereby implicitly includes all of the extender components' dynamics. Structured dynamic models, such as first- or second-order transfer functions that represent the dynamic behavior of the extender components (e.g., actuators or sensors), are thus avoided in the extender general analysis. These models, when used for control analysis, lead to very specific stability conditions that may not be applicable to all classes of extenders.

In the most general dynamic model for the extender, the extender position, y_e , is an $n_e \times 1$ vector resulting from two classes of inputs: first, the electronic command to the extender drive system, and second, the forces imposed on the extender. It is assumed that the extender primarily has

⁶Appropriate modification of the extender for this use would include decreasing the overall size of the extender, decreasing the size of the actuators used, and improving the cosmetic appearance of the extender.

⁷Myoelectric: Pertaining to the electric or electromotive properties of muscle.

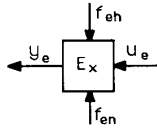


Fig. 2. Extender position, y_e , is function of input command signals, u_e , forces from the object being manipulated, f_{en} , and forces from human, f_{eh} . Arguments for all functions are omitted except when new functions are defined or when required for clarity.

either a closed-loop velocity controller or a closed-loop position controller. This is not the only controller on the extender; Section VI describes other feedback loops on the extender. Choosing a primary stabilizing compensator⁸ for the extender has been motivated by the following two issues.

- 1) It is important for human safety that the extender remain stable when not worn by a human. A closed-loop velocity controller or a closed-loop position controller keeps the extender stationary when not worn by a human.
- 2) The design of the primary stabilizing compensator lets the designers deal with the robustness of the extender without getting involved in the dynamics of the human and the object being manipulated by the extender.

The choice of a primary stabilizing compensator is not discussed here; a variety of compensators can be used to stabilize the system in the presence of uncertainties [9], [20]. Regardless of the type of primary stabilizing compensator, it is assumed that the extender position y_e is the extender model output, u_e is the input electronic command to the primary compensator, f_{eh} is the force imposed by the human on the extender, and f_{en} is the force imposed by the environment (the object being manipulated) on the extender. Equation (1) is an expression for the position of the extender, y_e . Fig. 2 shows the block diagram for the dynamic behavior of the extender.

$$y_e = E_x(u_e, f_{eh}, f_{en}) \quad (1)$$

If a position controller is selected to be the primary stabilizing compensator, mapping 1 is stable. However, if a velocity controller is selected to be the primary controller, the extender position is not a stable function of the extender inputs. The following norm inequality can be defined by taking the truncated L_2 norms of both sides of (1):

$$\|y_{e,T}\|_2 < \alpha_{ue}\|u_{e,T}\|_2 + \alpha_{feh}\|f_{eh,T}\|_2 + \alpha_{fen}\|f_{en,T}\|_2 + \beta_{ye} \quad \forall t \in T \quad (2)$$

⁸Hereafter, the words "primary stabilizing compensator" refer to either a closed-loop position controller or a closed-loop velocity controller that stabilizes the extender.

where α_{ue} , α_{feh} , α_{fen} , and β_{ye} are positive constants, and $y_{e,T}$, $u_{e,T}$, $f_{eh,T}$, and $f_{en,T}$ are the truncated functions.⁹ The extender "sensitivity" gain, α_{feh} , represents a mapping from the "size" of the human force, f_{eh} , to the "size" of the extender position, y_e . If α_{feh} is small, then the motion of the extender has a small response to the human force, f_{eh} . Similarly, α_{fen} is defined as the sensitivity of the extender motion to the environmental force, f_{en} . A closed-loop positioning system with several integrators as the extender primary controller yields small α_{fen} and α_{feh} , and consequently small extender response to f_{en} and f_{eh} .

IV. DYNAMIC BEHAVIOR OF THE HUMAN ARM

This section describes the dynamic behavior of the human arm as a relationship between inputs and outputs. Therefore there is less concern for the internal structure of the components in the model. The particular dynamics of nerve conduction, muscle contraction, and central nervous system processing are implicitly accounted for in constructing the dynamic model of the human arm.

Fundamental differences in human arm behavior can be attributed to two types of maneuvers: unconstrained and constrained. In unconstrained maneuvers, the human arm is driven in its workspace without contact with any environment. In constrained maneuvers, the human arm is driven in its workspace so the environment continuously exerts a dynamic constraint on the human arm. Since the human arm, wearing the extender, is always constrained by the extender, the primary focus is on constrained maneuvers.

This article avoids attributing a particular class of control action to constrained maneuvers of the human arm. It is not certain that the human arm behaves as a force-control system that accepts a set of command forces from the central nervous system. Maneuvering our hands in a stream of water from one point to another target point, while struggling with the water current, is an example that shows the human arm can work as a position control in a constrained space and can continuously accept a position or velocity command from the central nervous system. On the other hand, pushing a pin into a wall is an example of a constrained maneuver where the human imposes a force on the pin without being concerned about the pin position

⁹If $\|y_e\|_2 < \infty$, then $y_e \in L_2^T$ which implies that y_e is L_2^T -stable [21]. In cases where the norm may approach infinity, a truncated function $y_{e,T}$ is defined as

$$y_{e,T} = y_e, \quad t < T$$

$$y_{e,T} = 0, \quad t > T.$$

If $\|y_{e,T}\|_2 < \infty$, then y_e belongs to the extended L_2^T -space denoted by L_{2e}^T . This definition facilitates the analysis of systems in which the subsystems are unstable while the entire system may be stable. Although mapping 1 may not be L_2 stable, inequality 2 assumes that within any limited time, T , the extender position will be bounded whether the extender primary controller is a position controller or a velocity controller.

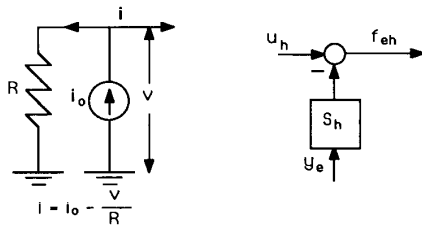


Fig. 3. Force imposed by human arm on extender. f_{eh} is function of commands from central nervous system, u_h , and extender position y_e .

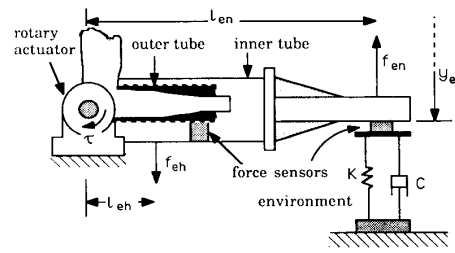
in the direction normal to the wall; this may be viewed as a system that accepts force commands from the central nervous system.

Considering the above dilemma in attributing a particular control action to constrained maneuvers of the human arm, a Norton or a Thevenin equivalent concept is used to arrive at a general substitute for the entire dynamic behavior of the human arm interacting with the extender. In the same way that the choice of a Norton or Thevenin equivalent does not affect the behavior of a circuit in interaction with other circuits, our choice in modeling the human arm by a Norton or a Thevenin equivalent has no effect on its interaction with other systems. Considering the "force-current" analogy between electrical and mechanical systems, a Norton equivalent is chosen to model the human arm dynamic behavior as a non-ideal source of force interacting with other systems. The notion of "non-ideal" indicates that this force-control system responds to both position disturbances from the extender and force commands from the central nervous system. Since the human arm is only in contact with the extender, the position and/or velocity disturbances on the human arm are only from the extender.

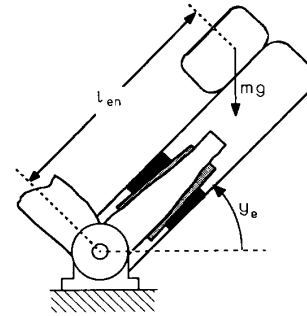
The force imposed by the human arm on the extender results from two inputs. The first input, u_h , is issued by the central nervous system, and the motion (position and/or velocity) of the extender forms the second input. One can think of the extender motion as a position disturbance occurring on the force-controlled human arm. If the extender is stationary, the force imposed on the extender is only a function of commands from the central nervous system. However, if the extender moves, the force imposed on the extender is a function not only of the central nervous system commands but also of the motion (velocity and/or position) of the extender. It is assumed that the specified form of u_h is not known other than that it is human thought deciding to impose a force onto the extender. If the extender moves, the imposed forces on the extender are different from u_h . S_h is defined in (3) to map the extender position, y_e , onto the imposed force on the object, f_{eh} . Thus

$$f_{eh} = u_h - S_h(y_e). \quad (3)$$

S_h , the human arm "sensitivity" operator, is the disturbance rejection property of the human arm. If the gain of S_h is small, then the extender motion has a small effect on



(a)



(b)

Fig. 4. (a) Amount of torque that constrains extender motion is counterclockwise torque of $(Ky_e + C\dot{y}_e)l_{en}^2$. (b) Amount of torque that constrains extender motion in free maneuver is clockwise torque of $[ml_{en}^2\ddot{y}_e + mgl_{en}\cos(y_e)]$.

the imposed forces, f_{eh} . Fig. 3 shows the Norton equivalent circuit and the block diagram of (3), where i , i_0 , v , and $1/R$ correspond to f_{eh} , u_h , y_e , and S_h , respectively. Since it is assumed that the human arm is stable, the following norm inequality can be defined by taking the L_2^n norms of both sides of (3):

$$\|f_{eh}\|_2 < \|u_h\|_2 + \alpha_{S_h}\|y_e\|_2 + \beta_{f_{eh}} \quad (4)$$

where α_{S_h} and $\beta_{f_{eh}}$ are positive constants.

V. DYNAMIC BEHAVIOR OF THE ENVIRONMENT

The extender is used either to manipulate heavy objects or to impose large forces on objects.¹⁰ A simple example of extender-environment interaction is seen in Fig. 4(a) in a single-degree-of-freedom extender prototype. This example shows the single-degree-of-freedom extender swinging clockwise, compressing an environmental apparatus. The deformation of the environment is equal to y_e , the position vector of the extender. Defining the direction of f_{en} as being to the extender from the environment, the torque that constrains the extender motion is a counterclockwise torque of $(K + Cs)l_{en}^2y_e$, where K , C , y_e , and s are stiffness, damping, extender angular orientation, and the Laplace operator, respectively. In another example, in Fig. 4(b), maneuvering an object with mass m and angular acceleration of \ddot{y}_e results in a constraining clockwise torque

¹⁰In this article, the word "environment" has also been used to represent any object being manipulated or pushed by the extender.

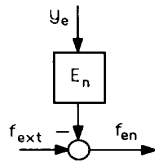


Fig. 5. General representation of environment dynamics.

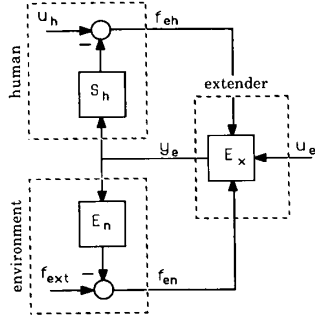


Fig. 6. Dynamics of extender, human, and environment without any feedback. This block diagram is composed of block diagrams of Figs. 2, 3, and 5.

of $[ml_{en}^2\ddot{y}_e + mgl_{en}\cos(y_e)]$, where y_e is the angular orientation of the extender.

Defining E_n as a nonlinear operator representing the environmental dynamics and f_{ext} as the equivalent of all the external forces imposed on the environment, (5) provides a general expression for the force on the extender, f_{en} , as a function of y_e :

$$f_{en} = -E_n(y_e) + f_{ext}. \quad (5)$$

In the example of a spring and damper (Fig. 4(a)), E_n is a transfer function such that $E_n(s) = (K + Cs)I_{en}^2$ and $f_{ext} = 0$. In the example of accelerating a mass (Fig. 4(b)), E_n is a nonlinear function such that $E_n(y_e) = [ml_{en}^2\ddot{y}_e + mgl_{en}\cos(y_e)]$ and $f_{ext} = 0$. Fig. 5 shows the general block diagram of the environmental dynamics. It is not clear if the environment is an L_2 stable function of y_e . Similar to the extender dynamic behavior, mapping 5 is assumed to be bounded within any bounded interval T . The following norm inequality can be defined by taking the L_2^n norms of both sides of (5):

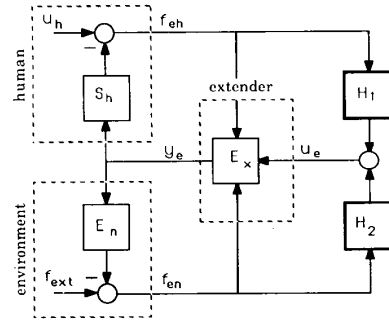
$$\|f_{en}, \tau\|_2 < \alpha_{En}\|y_e, \tau\|_2 + \|f_{ext}, \tau\|_2 + \beta_{fen} \quad \forall t \in T \quad (6)$$

where α_{En} and β_{fen} are positive constants.

VI. DYNAMIC MODEL OF THE HUMAN, EXTENDER, AND ENVIRONMENT

The dynamic behavior of the extender, human, and a load can be represented by the block diagram in Fig. 6, where (1), (3), and (5) are valid.

If u_e , u_h , and f_{ext} in Fig. 6 are zero (i.e., the input to the extender is zero, the human has no intention to move the extender, and no other forces are imposed on the extender), the interaction force between the human and extender is zero. If the human decides to move his hand (i.e., u_h


 Fig. 7. Compensators H_1 and H_2 increase apparent sensitivity of extender in response to forces from human and from environment.

becomes a nonzero value) and u_e and f_{ext} are still zero, a small extender motion develops from the interaction force between the human and extender. The extender motion is trivial if α_{feh} has a small gain, even though the interaction force may not be small. The human arm may not have the strength to overcome the extender primary control loop. The objective is to increase the effective strength of the human by increasing the apparent sensitivity of the extender. This can be done by using the interaction force as an input to the extender closed control loop as shown in Fig. 7. The interaction force is measured, then properly modified by compensator H_1 . At this point, there is no restriction on the structure and size of H_1 . The output of the compensator is used as an extender input command, u_e . Designers do not have complete freedom in choosing the structure and magnitude of H_1 since the closed-loop system must remain stable for any chosen value of H_1 . Compensator H_2 is also chosen to generate extender compliancy in response to the forces on the extender endpoint [11], [12]. In the next section, the role of H_1 and H_2 in the performance of the extender is described.

VII. PERFORMANCE

This section addresses the following question: What dynamic behavior should the extender have in performing a task? The resulting performance specification does not assure the stability of the system in Fig. 7 but does let designers express what they wish to have happen during a maneuver if instability does not occur. (Sections VIII and IX show that designers must accept a trade-off between performance and closed-loop stability.) The following example describes a performance specification for the extender.

Suppose the extender is employed to manipulate an object through a completely arbitrary trajectory.¹¹ It is reasonable to ask for an extender dynamic behavior where the human feels the scaled-down values of the forces on the extender: that is, the human has a natural sensation of the forces required to maneuver the load. In other words,

¹¹For clarity in understanding the concept of performance, it is assumed that f_{ext} on the object is zero. The equations derived in this section can be extended to cases where f_{ext} is not zero.

the human would feel the scaled-down values of the acceleration, centrifugal, coriolis, and gravitational forces associated with an arbitrary maneuver. This example calls for masking the dynamic behavior of the extender, human, and load via the design of H_1 and H_2 such that a desired relationship is guaranteed between f_{eh} and f_{en} . Without any proof, it is stated that only one relationship between two variables (among three variables f_{eh} , f_{en} , and y_e) is needed to specify a unique behavior for the extender. Note that (5) has already established a relationship between f_{en} and y_e via E_n when $f_{ext} = 0$. If one relationship between f_{en} and f_{eh} is specified, then other relationships (for example, one between f_{eh} and y_e) cannot be specified. This is true because substituting for f_{en} from (5) into the specified relationship between f_{en} and f_{eh} results in a relationship between y_e and f_{eh} . Therefore the objective is to choose H_1 and H_2 so that one relationship can be established between f_{eh} and f_{en} or between f_{eh} and y_e . The following equations are suggested as the two target relationships:

$$f_{eh} = P(f_{en}) \quad (7)$$

$$f_{eh} = R(y_e). \quad (8)$$

$P(\cdot)$ and $R(\cdot)$ are arbitrary nonlinear target dynamics. The first equation, which is the most natural design specification for extenders, allows the designers to specify a relationship between the forces f_{eh} and f_{en} . The second relationship establishes an impedance for the extender. The following describes two design examples in which one of the design specifications ((7) or (8)) is of interest.

A. Shaping the Force

Suppose the purpose is to guarantee a relationship between the forces f_{eh} and f_{en} (as in (7)). A trajectory controller can be designed so that α_{fen} and α_{feh} are small gains and E_x creates an approximately unity gain from u_e to y_e . This can be achieved by implementing a position controller that creates a large open-loop gain in the extender itself. For example, if several integrators are used in the extender primary controller, then α_{feh} and α_{fen} are small, which results in small extender response to f_{eh} and f_{en} . The governing dynamic equation when the primary controller is insensitive to f_{eh} and f_{en} is

$$y_e \approx H_1(f_{eh}) + H_2(f_{en}). \quad (9)$$

H_1 and H_2 are chosen as

$$H_1(f_{eh}) = 2E_n^{-1}(-P^{-1}(f_{eh})) \quad (10)$$

$$H_2(f_{en}) = -E_n^{-1}(-f_{en}). \quad (11)$$

$E_n^{-1}(-f_{en})$ is the solution of the environment dynamic equation for a given $-f_{en}$; y_e must be calculated from (5) for any given $-f_{en}$. Substituting H_1 and H_2 ((10) and (11)) into (9) results in

$$y_e \approx -E_n^{-1}(-f_{en}) + 2E_n^{-1}(-P^{-1}(f_{eh})). \quad (12)$$

Since $y_e = E_n^{-1}(-f_{en})$, then

$$E_n^{-1}(-f_{en}) \approx -E_n^{-1}(-f_{en}) + 2E_n^{-1}(-P^{-1}(f_{eh})) \quad (13)$$

and, consequently

$$f_{eh} \approx P(f_{en}). \quad (14)$$

In an example illustrating the preceding case, an extender is used to hold a jackhammer. The objective is to decrease and filter the force transferred to the human arm so the human feels only the low-frequency force components. This requires that $f_{eh} = -\alpha M(s)f_{en}$ where, preferably, $M(s)$ is a diagonal matrix with low-pass filter transfer functions as members. α is a scalar smaller than unity and represents the force reduction. Choosing $P(s) = -\alpha M(s)$, the required forms of H_1 and H_2 are as follows:

$$H_1(f_{eh}) = 2E_n^{-1}\left(\frac{1}{\alpha}M^{-1}(s)f_{eh}\right) \quad (15)$$

$$H_2(f_{en}) = -E_n^{-1}(-f_{en}). \quad (16)$$

Substituting H_1 and H_2 from (15) and (16) into (9) results in $f_{eh} \approx -\alpha M(s)f_{en}$. The preceding method calls for the class of P functions that are exactly invertible or at least can be inverted approximately. For example, if $M(s)$ is chosen as a first-order filter, then $M^{-1}(s)$ in (15) can be realized for a bounded frequency range.

B. Shaping the Impedance

Suppose the purpose is to guarantee a relationship between the forces f_{eh} and y_e (8) without any regard to the relationship between f_{eh} and f_{en} . Again, a trajectory controller can be designed so that α_{fen} and α_{feh} have very small gains and E_x creates an approximate unity gain from u_e to y_e . Therefore (9) governs the dynamic behavior of the system. Suppose H_1 and H_2 are chosen such that

$$H_1(f_{eh}) = 2R^{-1}(f_{eh}) \quad (17)$$

$$H_2(f_{en}) = -E_n^{-1}(-f_{en}). \quad (18)$$

Substituting H_1 and H_2 from (17) and (18) into (9) results in

$$y_e \approx -E_n^{-1}(-f_{en}) + 2R^{-1}(f_{eh}). \quad (19)$$

Since $y_e = E_n^{-1}(-f_{en})$, then (19) results in

$$y_e \approx R^{-1}(f_{eh}). \quad (20)$$

Equation (20) guarantees that the target impedance in (8) has been achieved.

In an example for this case, the goal is to feel the forces resulting from maneuvering a point mass when maneuvering a rigid body. This behavior requires masking the cross-coupled forces associated with rigid body maneuvers. This behavior is characterized by $f_{eh} = D(s)y_e$, where $D(s)$ is a diagonal matrix with second-order functions as members and s is the Laplace operator. For a two-dimensional maneuver, $D(s)$ is shown in (21), where m_1 and m_2 are chosen to be the "apparent masses" in two directions:

$$D(s) = \begin{pmatrix} m_1 s^2 & 0 \\ 0 & m_2 s^2 \end{pmatrix}. \quad (21)$$

Equation (21) guarantees a natural sensation of the forces used to maneuver a point mass. Choosing $H_1(s) = 2D^{-1}(s)$ and $H_2(f_{en}) = -E_n^{-1}(-f_{en})$, and substituting them in (9), results in $f_{eh} \approx D(s)y_e$.

VIII. CLOSED-LOOP STABILITY

A sufficient condition for stability of the closed-loop system of Fig. 7 is developed by the small gain theorem. This sufficient condition results in a class of compensators which guarantee the stability of the closed-loop system in Fig. 7. Note that the stability condition derived in this section does not give any indication of system performance, but only ensures a stable system. This stability condition also clarifies the trade-off between performance and closed-loop stability. (See [21] to understand the mathematical notation used in this analysis.) Suppose H_1 and H_2 are chosen as nonlinear operators such that $H_1, H_2: L_2^n \rightarrow L_2^n$ and

$$\|H_1(f_{eh}, \tau)\|_2 < \alpha_{H1}\|f_{eh}, \tau\|_2 + \beta_{H1} \quad (22)$$

$$\|H_2(f_{en}, \tau)\|_2 < \alpha_{H2}\|f_{en}, \tau\|_2 + \beta_{H2} \quad (23)$$

where α_{H1} , α_{H2} , β_{H1} , and β_{H2} are positive constants. Since $u_e = H_1(f_{eh}) + H_2(f_{en})$:

$$\|u_e\|_2 < \alpha_{H1}\|f_{eh}, \tau\|_2 + \alpha_{H2}\|f_{en}, \tau\|_2 + \beta_{H1} + \beta_{H2}. \quad (24)$$

Substituting $\|f_{eh}, \tau\|_2$, $\|f_{en}, \tau\|_2$, $\|u_e, \tau\|_2$ from inequalities (4), (6), and (24) into inequality (2) results in inequality (25) for $\|y_e\|_2$:

$$\begin{aligned} \|y_e\|_2 < & (\alpha_{feh}\alpha_{Sh} + \alpha_{fen}\alpha_{En} + \alpha_{ue}\alpha_{H1}\alpha_{Sh} + \alpha_{ue}\alpha_{H2}\alpha_{En}) \\ & \cdot \|y_e\|_2 + (\alpha_{H1}\alpha_{ue} + \alpha_{feh})\|u_h\|_2 \\ & + (\alpha_{H2}\alpha_{ue} + \alpha_{fen})\|f_{ext}\|_2 \\ & + (\alpha_{feh} + \alpha_{ue}\alpha_{H1})\beta_{feh} + (\alpha_{fen} + \alpha_{ue}\alpha_{H2})\beta_{fen} \\ & + \alpha_{ue}(\beta_{H1} + \beta_{H2}) + \beta_{ye}. \end{aligned} \quad (25)$$

Employing the small gain theorem, the closed-loop system of Fig. 7 is L_2 stable if

$$\alpha_{feh}\alpha_{Sh} + \alpha_{fen}\alpha_{En} + \alpha_{ue}\alpha_{H1}\alpha_{Sh} + \alpha_{ue}\alpha_{H2}\alpha_{En} < 1. \quad (26)$$

Inequality (26) expresses the stability condition of the closed-loop system in Fig. 7. By inspection of inequality (26), it can be observed that the smaller are H_1 and H_2 , the larger is the stability range. To illustrate the trade-off between stability and performance, a simple case is considered where a high gain positioning system is designed as the primary compensator such that α_{fen} and α_{feh} are rather small. The stability condition for small α_{fen} and α_{feh} reduces to

$$\alpha_{ue}\alpha_{H1}\alpha_{Sh} + \alpha_{ue}\alpha_{H2}\alpha_{En} < 1. \quad (27)$$

H_1 and H_2 represent the performance of the system. For example, when a larger H_1 is chosen for (15) (by choosing a smaller α), a larger torque amplification can be achieved. Designers, however, may not freely select H_1 : inequality (27) must also be guaranteed. If α_{En} is chosen to be zero,

the stability condition applies to free maneuvers when the robot is not in contact with any object:

$$\alpha_{ue}\alpha_{H1}\alpha_{Sh} < 1. \quad (28)$$

Inequality (28) states that guaranteeing stability of the closed-loop system requires some initial compliancy in the human arm. If the human hand has a large sensitivity to position disturbances (i.e., it rejects position disturbances by moving very quickly), then the system stability can be guaranteed by a small H_1 . Large S_h implies a stiff human arm and, theoretically, as $\alpha_{Sh} \rightarrow \infty$, the stability of the closed-loop system can no longer be guaranteed. More trade-offs between performance and stability are described in Section IX.

IX. CLOSED-LOOP STABILITY (LINEAR ANALYSIS)

Using transfer function matrices, the linear dynamic behavior of the extender, human, and environment can be described by (29), (30), and (31):

$$y_e = G_e(s)u_e + S_{eh}(s)f_{eh} + S_{en}(s)f_{en} \quad (29)$$

$$f_{en}(s) = -E_n(s)y_e + f_{ext} \quad (30)$$

$$f_{eh} = -S_h(s)y_e + u_h \quad (31)$$

where G_e represents the closed-loop transfer function for the extender and S_{eh} and S_{en} represent the extender sensitivity transfer functions in response to forces f_{eh} and f_{en} . Using the multivariable Nyquist theorem, inequality (32) can be used for the stability analysis [8], [13]:

$$\sigma_{\max}(G_e H_1 S_h + G_e H_2 E_n) < \sigma_{\min}(I + S_{eh} S_h + S_{en} E_n) \quad \text{for all } \omega \in (0, \infty). \quad (32)$$

If a high gain positioning system is designed as the primary compensator for the extender, then S_{en} and S_{eh} are rather small, and the stability condition reduces to

$$\sigma_{\max}(G_e H_1 S_h + G_e H_2 E_n) < 1 \quad \text{for all } \omega \in (0, \infty). \quad (33)$$

Inequality (33) is similar to inequality (27). For a single-degree-of-freedom extender, the stability condition of (32) reduces to

$$|G_e H_1 S_h + G_e H_2 E_n| < |1 + S_{eh} S_h + S_{en} E_n| \quad \text{for all } \omega \in (0, \infty). \quad (34)$$

If H_2 is chosen to be zero, then

$$|H_1| < \frac{1}{|G_e|} \left| S_{eh} + \frac{1}{S_h} + \frac{S_{en} E_n}{S_h} \right| \quad \text{for all } \omega \in (0, \infty). \quad (35)$$

If the extender is not in contact with any load ($E_n = 0$), the stability condition reduces to

$$|H_1| < \frac{1}{|G_e|} \left| S_{eh} + \frac{1}{S_h} \right| \quad \text{for all } \omega \in (0, \infty). \quad (36)$$

Inequality (36) states that, to guarantee the stability of the closed-loop system, there must be some initial compliancy in either the human arm, $1/S_h$, or the extender primary

control system, S_{eh} . Loosely speaking, S_h represents the human hand stiffness. The system stability cannot be guaranteed if S_{eh} is very small (i.e., a stiff extender) and the human hand has infinite sensitivity to position disturbances (i.e., the human hand has a very large S_h and it does not reject position disturbances by moving very quickly). Inequality (36) also shows that the system has a smaller stability range when no load is in contact with the extender. Therefore, if the extender is stable without any load, it is also stable for all possible values of the environment dynamics.

According to the results of Section VII, the performance of the extender is determined by the chosen values of H_1 . The larger H_1 is chosen to be, the smaller the ratio of f_{eh} to f_{en} is. Loosely speaking, large H_1 allows the human to manipulate large objects or to impose large forces onto the environment. On the other hand, the stability conditions given above require small values for H_1 to guarantee the stability of the system. This trade-off between stability and performance is illustrated experimentally in the next sections.

X. EXPERIMENTAL ANALYSIS

A single-degree-of-freedom extender (Fig. 8) is used to verify experimentally the theoretical predictions for extender stability and performance. This experimental extender consists of an outer tube and an inner tube (Fig. 4(a)). The human arm, wrapped in a cylinder of rubber for a snug fit, is located in the inner tube. A piezoelectric load cell, placed between these tubes, measures the interaction force between the human arm and the extender, f_{eh} . Another piezoelectric force cell, set between the extender and the environment, measures the interaction force between the extender and environment, f_{en} . A rotary hydraulic actuator, mounted on a solid platform, powers the outer tube of the extender. The actuator shaft, supported by two bearings, is connected to the outer tube to transfer power. In addition to the piezoelectric load cells, other sensing devices include a tachometer and an encoder (with a corresponding counter) to measure the angular speed and position of the motor shaft. An automobile strut, mounted on a custom fixture below the extender, is the experimental environment. An IBM/AT computer is used for data acquisition and control. Based on the information from these sensors, a control algorithm calculates a command signal, which is sent to the extender servo controller board via a digital-to-analog (D/A) converter.

Fig. 9 shows a position controller as the primary stabilizing controller for the extender. The closed-loop position controller, $G_e(s)$, from u_e to the extender position y_e , is governed by position and velocity feedback gains. $G_p(s)$ and $G_d(s)$ are the transfer functions of the open-loop extender that show how the extender responds to the input current, i , and the forces, f_{en} and f_{eh} . The moment arm l_{eh} , representing the effect of the human force, is about one-third of l_{en} . The servo-controller board, with a gain of K_b , outputs a current proportional to the command volt-

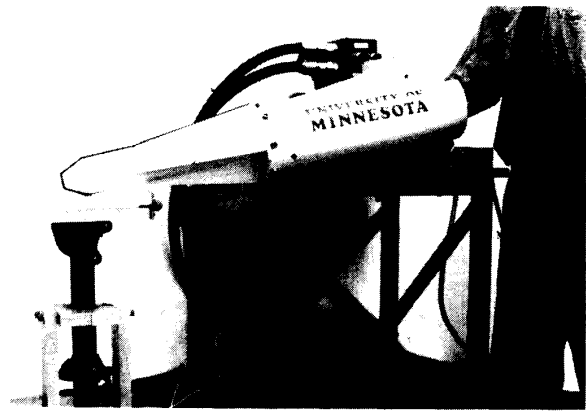


Fig. 8. Experimental extender.

age, resulting in a displacement of the servovalve spool. The extender velocity is measured for feedback by a tachometer with a gain of K_t and is fed to the computer by an analog-to-digital converter with a gain of K_{ad} . The extender position is measured by an encoder via a parallel I/O board with a gain of K_{IO} . The precompensator K_o is used as a constant gain to change the input units. K_1 and K_2 are position and velocity gains and K_{da} is the digital-to-analog converter gain.

Equations (37) and (38) are the experimentally verified transfer functions for G_p and G_d . Appendix A describes their detailed theoretical and experimental derivations:

$$G_p = \frac{y_e}{i} = \frac{355}{s \left(\frac{s^2}{1560.25} + \frac{s}{43.89} + 1 \right)} \quad \text{rad/A} \quad (37)$$

$$G_d = 135 \times 10^{-7} \frac{\frac{s}{23.6} + 1}{s \left(\frac{s^2}{1560.25} + \frac{s}{43.89} + 1 \right)} \quad \text{rad/(lbf} \cdot \text{in)}. \quad (38)$$

Using $K_1 = 0.94$ and $K_2 = 0.00977$ yields the widest bandwidth for the closed-loop transfer function, G_e , and guarantees the stability of the system in the presence of bounded unmodeled dynamics in the extender [9]. From Fig. 9, an expression for G_e is derived in (39). Fig. 10 depicts the theoretical and experimental values for the Bode plot of G_e :

$$G_e = \frac{y_e}{u_e} = \frac{1}{\frac{s^3}{18860} + \frac{s^2}{530.52} + \frac{s}{11.83} + 1} \quad \text{rad/rad}. \quad (39)$$

S_{en} is defined as the sensitivity of the extender position y_e to f_{en} applied at a moment arm of $l_{en} = 3'$. S_{eh} is defined as the sensitivity of the extender position to f_{eh} applied at a moment arm of $l_{eh} = 1'$. By inspecting the block diagram of Fig. 9 and substituting the parameter values, S_{en} can be

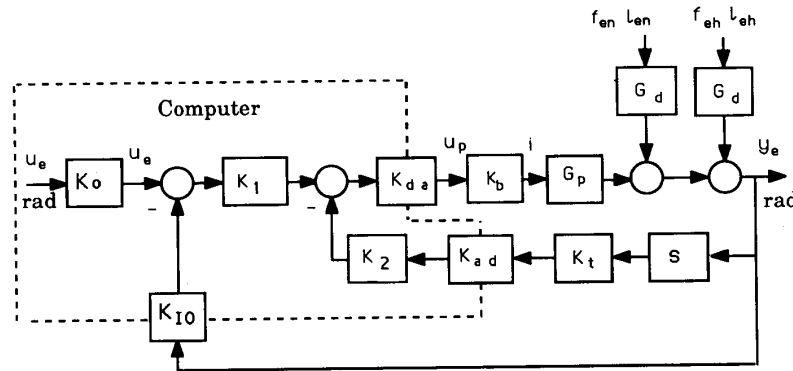


Fig. 9. Block diagram of closed-loop position controller. tachometer gain: $K_t = 0.169 \text{ V}/(\text{rad}/\text{s})$; servo-controller board gain: $K_b = 0.00465 \text{ A}/\text{V}$; digital-to-analog converter: $K_{da} = 10 \text{ V}/2048$; analog-to-digital converter: $K_{ad} = 2048/1.25 \text{ V}$; parallel IO gain: $K_{IO} = 1592 \text{ number}/\text{rad}$; precompensator gain: $K_p = 1592 \text{ number}/\text{rad}$; position gain: $K_1 = 0.94$; velocity gain: $K_2 = 0.00977$.

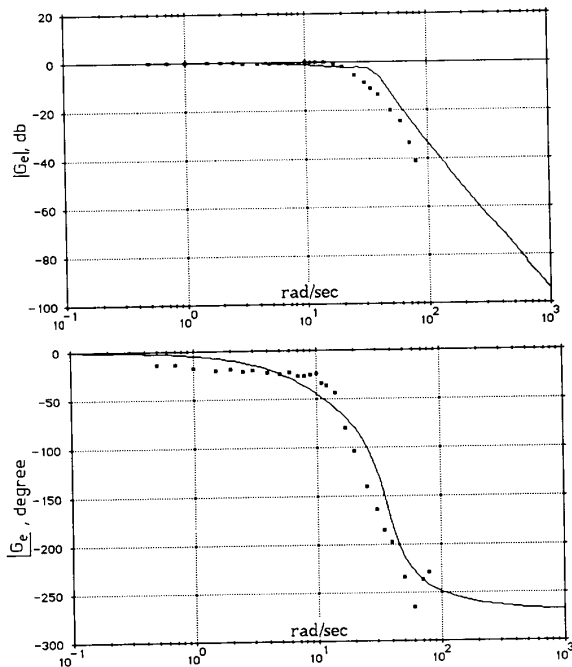


Fig. 10. Experimental and theoretical Bode plot of G_e . Extender closed-loop position has bandwidth of about 10 rad/s.

found as follows:

$$S_{en} = \frac{y_e}{f_{en}} = 0.00004 \frac{\frac{s}{23.6} + 1}{\frac{s^3}{18860} + \frac{s^2}{530.52} + \frac{s}{11.83} + 1} \text{ rad/lbf.} \quad (40)$$

Since the human arm force affects the extender about three times less than the environment force, S_{eh} is about

three times less than S_{en} :

$$S_{eh} = \frac{l_{eh}}{l_{en}} S_{en} = 1.34 \times 10^{-5} \frac{\frac{s}{23.6} + 1}{\frac{s^3}{18860} + \frac{s^2}{530.52} + \frac{s}{11.83} + 1} \text{ rad/lbf.} \quad (41)$$

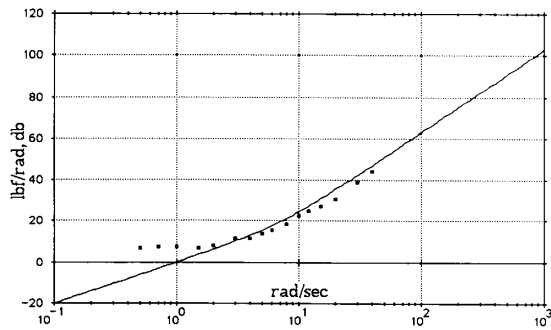
XI. ENVIRONMENT DYNAMIC ANALYSIS

An automobile strut, mounted on a custom fixture below the extender, is the experimental environment (Fig. 4(a)). This environment can be modeled as a linear spring and damper system, where inertial effects of the strut are negligible compared to the spring and damping effects. The environmental stiffness and damping are measured to be 2050 lbf/rad and 200 lbf/(rad/s), where radians represent the angular displacement of the motor shaft. A dynamic value for E_n is given in (42), where the bandwidth of 10 rad/s can be observed:

$$E_n = 200s + 2050 \text{ lbf/rad.} \quad (42)$$

XII. HUMAN-ARM DYNAMIC ANALYSIS

The model derived here does not represent human arm sensitivity, S_h , for all configurations; it is only an approximate and experimentally verified model of the author's elbow in the neighborhood of the Fig. 4(a) configuration. The extender motion y_e , in the case of this prototype, is a rotating motion about the elbow joint. If the human elbow behaves linearly in the neighborhood of the horizontal position, S_h is the human arm impedance. For the experiment, the author's elbow was placed in the extender, and the extender was commanded to oscillate via sinusoidal functions. At each frequency of the extender oscillation, the operator tried to move his hand and follow the extender so that zero contact force was created between his hand and the extender. Since the human arm cannot keep up with the high-frequency motion of the extender when

Fig. 11. Experimental and theoretical plot of S_h .

trying to create zero contact forces, large contact forces and, consequently, a large S_h are expected at high frequencies. Since this force is equal to the product of the extender acceleration and human arm inertia (Newton's Second Law), at least a second-order transfer function is expected for S_h at high frequencies. On the other hand, at low frequencies (in particular at dc), since the operator can comfortably follow the extender motion, he can always establish almost zero contact forces between his hand and the extender. This leads to the assumption of a free derivative transfer function for S_h at low frequencies, where contact forces are small for all values of extender position. Based on several experiments at various frequencies, the best estimate for the author's hand sensitivity is presented by (43):

$$S_h = 0.143 s^2 + s \text{ lbf/rad.} \quad (43)$$

Since at low frequencies, particularly at dc, the human can usually create zero-contact forces, (43) does not contain any nonzero dc gain. Fig. 11 shows the experimental values and fitted transfer function for the human-hand dynamic behavior.

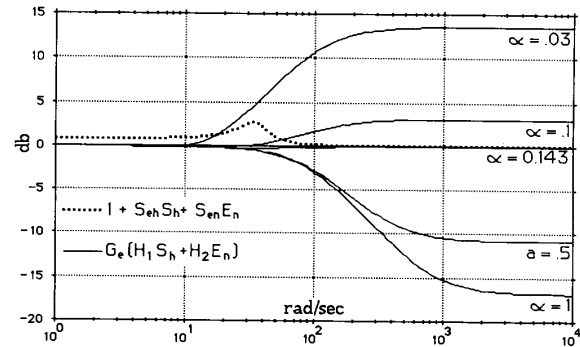
XIII. EXPERIMENTAL VERIFICATION OF STABILITY AND PERFORMANCE

The design objective is to decrease the force transferred to the human arm so the human feels the scaled-down values of the force imposed by the environment. This requires that $f_{eh} = -\alpha f_{en}$ where α is a scalar smaller than unity and represents the reduction of the force transmitted to the human arm. Using (15) and (16), H_1 and H_2 can be written as

$$H_1 = \frac{2}{\alpha E_n G_e} \quad (44)$$

$$H_2 = \frac{1}{E_n G_e}. \quad (45)$$

Substituting G_e and E_n from (39) and (42) into (44) and

Fig. 12. Inequality (34) (stability condition) is satisfied for $\alpha > 0.143$.

(45) gives H_1 and H_2 :

$$H_1 = \frac{2}{\alpha} \frac{s^3 + \frac{s^2}{18860} + \frac{s}{530.52} + 1}{(200s + 2050)} \quad (46)$$

$$H_2 = \frac{s^3 + \frac{s^2}{18860} + \frac{s}{530.52} + 1}{(200s + 2050)}. \quad (47)$$

Equations (46) and (47) are improper transfer functions. For implementation on the computer, two high-frequency poles are added to each of the transfer functions of (46) and (47).¹² The above values of H_1 and H_2 result in $f_{eh} = -\alpha f_{en}$. The designer cannot arbitrarily choose α ; to guarantee system stability, α must be chosen to guarantee inequality (34). However, if α is small (large force amplification), inequality (34) is violated at some frequencies, and no conclusion about stability can be made. Fig. 12, depicting both sides of inequality (34), shows that for guaranteed stability of the closed-loop system, α must be larger than 0.143.

In the first set of experiments, α is chosen to be 0.5 to satisfy inequality (34), and it is shown that the closed-loop system is stable. The basic procedure for the experiment consisted of using the prototype extender to push on the fabricated environment in a series of periodic functions. The forces f_{eh} and f_{en} were measured and recorded in data files. The recorded f_{eh} was used as an input to a computer simulation encompassing the dynamic behavior of the extender, human, and environment. Fig. 13 shows the simulated and experimental values of f_{en} along with the recorded value of f_{eh} for three different maneuvers when α is chosen to be 0.5 (twice force amplification). The experimental data and theoretical predictions are in close agreement. The first two plots are obtained using a low-frequency human arm motion. This demonstrates the linearity between the input f_{eh} and the output f_{en} . Note that

¹² H_1 and H_2 are divided by the force sensor and the A/D converter gains.

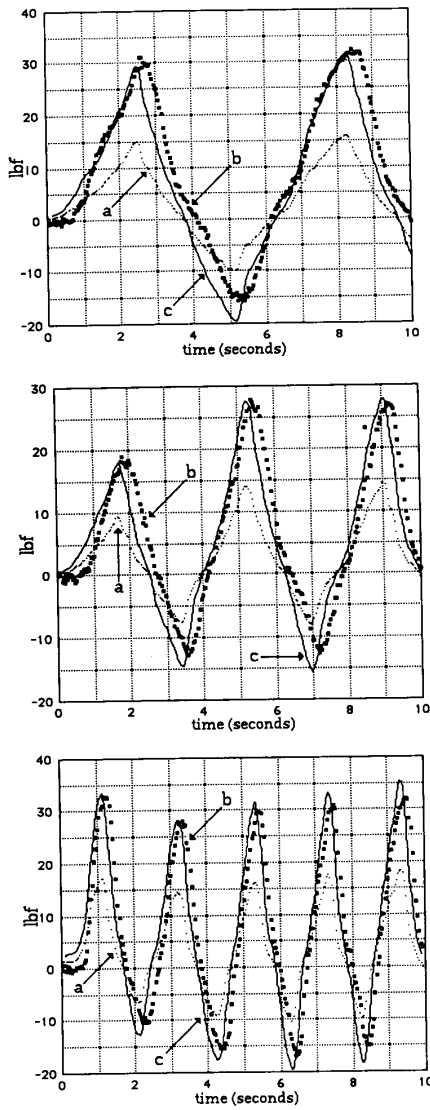


Fig. 13. Stable maneuver with $\alpha = 0.5$ (twice force amplification). (a) f_{eh} . (b) Experimental f_{en} . (c) Simulated f_{en} .

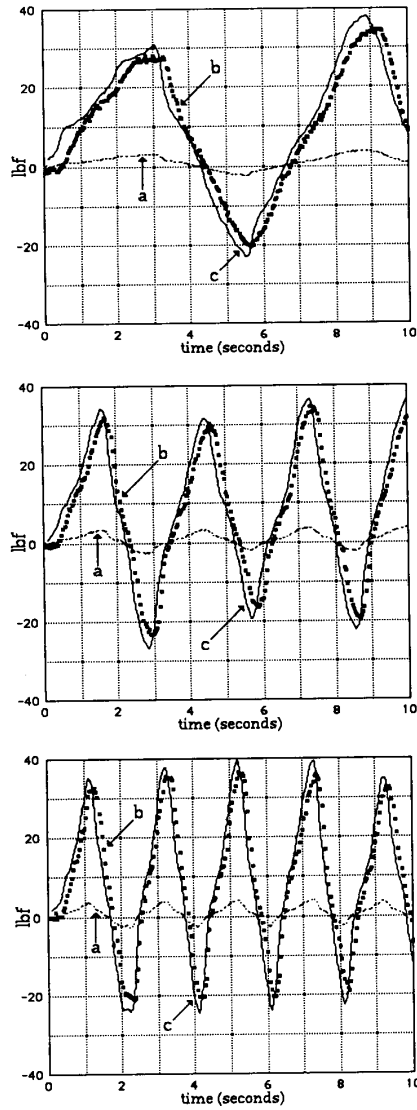


Fig. 15. With $\alpha = 0.1$ (ten times force amplification). H_1 and H_2 violate stability condition; however, system is stable. (a) f_{eh} . (b) Experimental f_{en} . (c) Simulated f_{en} .

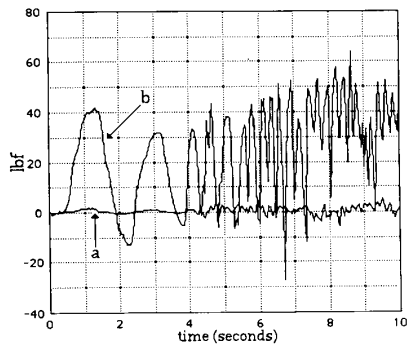
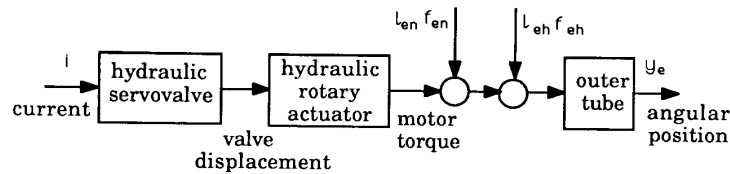
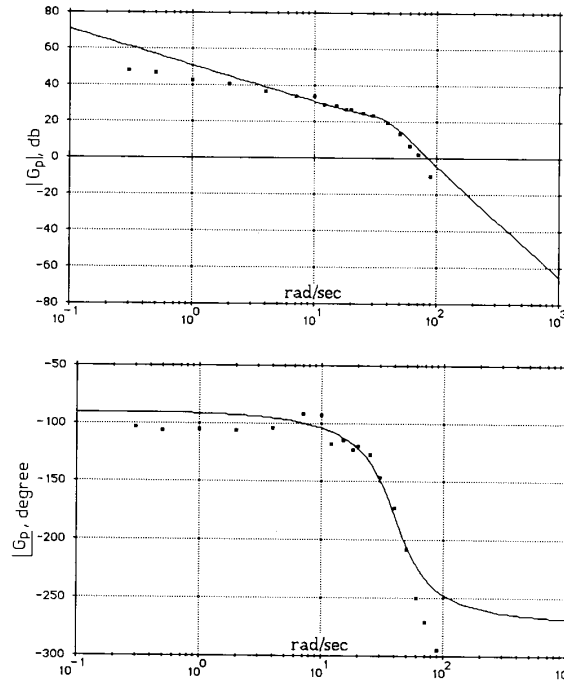


Fig. 14. Unstable maneuver with $\alpha = 0.03$ (30 times force amplification). H_1 and H_2 violate inequality (34). (a) f_{eh} . (b) Experimental f_{en} .

the output force f_{en} is consistently twice the input force f_{eh} . The second set of experiments was conducted with $\alpha = 0.03$, where the system exhibits instability in the form of oscillations (Fig. 14). Inspection of Fig. 12 shows that the choice of $\alpha = 0.03$ violates inequality (34). The trade-off between performance and stability can be observed here: the better the required performance (larger force amplification in this experiment), the narrower is the stability range. Since inequality (34) is only a sufficient condition for stability, violation of this condition does not lead to any conclusion. Fig. 15 shows the experimental and simulated contact forces when $\alpha = 0.1$ (force amplified by a factor of 10). The system is stable and f_{en} is consistently ten times larger than the force f_{eh} , but the stability condition is not satisfied.

Fig. 16. Internal block diagram of G_p .Fig. 17. Experimental data and theoretical G_p .

XIV. CONCLUSION

This paper discusses constrained motion in a class of human-controlled robotic manipulators called extenders. Extenders amplify the strength of the human operator while utilizing the intelligence of the operator to spontaneously generate the command signal to the system. A single-degree-of-freedom extender has been built for theoretical and experimental verification of the extender dynamics and control. System performance is defined as amplification of human force. It is shown that the greater the required amplification, the smaller is the stability range of the system. A condition for stability of the closed-loop system (extender, human and environment) is derived, and through both simulation and experimentation, the sufficiency of this condition is demonstrated.

APPENDIX A

Fig. 16 shows the internal block diagram of the open-loop extender. The current, i , is the command input to the hydraulic servovalve which allows the flow of hydraulic fluid to the rotary actuator. f_{eh} and f_{en} are the forces

imposed on the extender by the human and by the environment.

The dynamics of the hydraulic servovalve and rotary actuator system are described by equations (48), (49), and (A3) [15]:

$$Q_l = K_q i - K_p P_l \quad \text{valve equation} \quad (48)$$

$$Q_l = \frac{dy_e}{dt} D_m + \frac{V_t}{4\beta_e} \frac{dP_l}{dt} \quad \text{flow continuity equation} \quad (49)$$

$$P_l D_m + f_{en} l_{en} + f_{eh} l_{eh} = J \frac{d^2 y_e}{dt^2} \quad \text{Newton's Law} \quad (50)$$

where f_{en} , l_{en} , f_{eh} , and l_{eh} are defined in Fig. 4(a), and the other parameters are as follows:

- Q_l load flow, in³/s,
- K_q flow gain, (in³/s)/A,
- i current to drive servovalve, A,
- K_p pressure gain, in⁵/(s lbf),
- P_l load pressure, psi,
- y_e angular position of the extender, rad,
- D_m actuator volumetric displacement, 7.62 in³/rad,

J outer tube moment of inertia, 38.8 in-lbf-s²,
 β_e hydraulic fluid modulus of elasticity, 100000 psi,
 V_t total contained volume in actuator, 13.3 in³.

Eliminating P_l and Q_l from (48)–(50) gives (A4), a transfer function for the angular position of the open-loop extender, y_e :

$$y_e = G_p i + G_d f_{en} l_{en} + G_d f_{eh} l_{eh} \quad (51)$$

where

$$G_p = \frac{K_q}{D_m} \frac{1}{s \left(\frac{s^2}{\omega_e^2} + \frac{2\zeta_e s}{\omega_e} + 1 \right)},$$

$$G_d = \frac{K_p}{D_m^2} \frac{\frac{V_r s}{4\beta_e K_p} + 1}{s \left(\frac{s^2}{\omega_e^2} + \frac{2\zeta_e s}{\omega_e} + 1 \right)} \quad \text{and}$$

$$\omega_e = D_m \sqrt{\frac{4\beta_e}{V_t J}}, \quad \zeta_e = \frac{K_p}{D_m} \sqrt{\frac{\beta_e J}{V_t}}$$

By fitting G_p into an experimentally derived Bode plot (Fig. 17), the following parameters are derived:

$$\frac{K_q}{D_m} = 355 \text{ (rad/s)/A,}$$

$$\omega_e = 39.5 \text{ rad/s,}$$

$$\zeta_e = 0.45.$$

Using the preceding data, G_p is given by (52):

$$G_p = \frac{355}{s \left(\frac{s^2}{1560.25} + \frac{s}{43.89} + 1 \right)} \text{ rad/A.} \quad (52)$$

K_p/D_m^2 was determined to be 135×10^{-7} (rad/s)/(lbf·in). Using the values stated for V_t , β_e , and D_m , the numerical value for G_d is given by (53):

$$G_d = 135 \times 10^{-7} \frac{\frac{s}{23.6} + 1}{s \left(\frac{s^2}{1560.25} + \frac{s}{43.89} + 1 \right)} \text{ rad/(lbf·in).} \quad (53)$$

REFERENCES

[1] C. K. Battyke, A. Nightingale, and J. Whilles, Jr., "The use of myoelectric currents in the operation of prostheses," *J. Bone Joint Surg.*, vol. 37B.

[2] D. C. Clark *et al.*, "Exploratory investigation of the man-amplifier concept," U.S. Air Force Rep. AMRL-TDR-62-89, AD-390070, Aug. 1962.
 [3] R. W. Correll and M. J. Wijnschenck, "Design and development of the Case research arm aid," Engineering Design Center Rep. 4, Case Institute of Technology, Apr. 1964.
 [4] GE Company, "Exoskeleton prototype project, final report on phase I," Rep. S-67-1011, Schenectady, NY, 1966.
 [5] —, "Hardiman I prototype project, special interim study," Rep. S-68-1060, Schenectady, NY, 1968.
 [6] P. F. Groshaw, "Hardiman I arm test, Hardiman I prototype," Rep. S-70-1019, GE Company, Schenectady, NY, 1969.
 [7] J. M. Hollerbach, "A recursive lagrangian formulation of manipulator dynamics and a comparative study of dynamics formulation complexity," *IEEE Trans. Syst. Man Cybern.*, vol. 10, no. 11, pp. 730–736, Nov. 1980.
 [8] H. Kazerooni, "Human machine interaction via the transfer of power and information signals," *IEEE Int. Conf. on Robotics and Automation*, May 1989, Scottsdale, AZ, pp. 1632–1642.
 [9] —, "Loop shaping design related to LQG/LTR for SISO minimum phase plants," *Int. J. Contr.*, vol. 48, no. 1, July 1988.
 [10] —, "On the robot compliant motion control," *ASME J. Dynam. Syst. Measur. Contr.*, vol. 111, no. 3, Sept. 1989.
 [11] —, "Statically balanced direct drive robot manipulator," *Robotica*, vol. 7, no. 2, Apr. 1989.
 [12] H. Kazerooni, T. B. Sheridan, P. K. Houpt, "Robust compliant motion for manipulators," *IEEE Trans. Robot. Automat.*, vol. 2, no. 2, June 1986.
 [13] N. A. Lehtomaki, N. R. Sandell, M. Athans, "Robustness results in linear-quadratic Gaussian based multivariable control designs," *IEEE Trans. Auto. Contr.*, vol. AC-26, no. 1, pp. 75–92, Feb. 1981.
 [14] B. J. Makinson, "Research and development prototype for machine augmentation of human strength and endurance, Hardiman I project," Rep. S-71-1056, General Electric Co., Schenectady, NY, 1971.
 [15] H. E. Merritt, *Hydraulic Control Systems*. New York: John Wiley & Sons, Inc., 1967.
 [16] N. J. Mizen, "Preliminary design for the shoulders and arms of a powered, exoskeletal structure," Cornell Aeronautical Lab. Rep. VO-1692-V-4, 1965.
 [17] R. S. Mosher, "Force reflecting electrohydraulic servomanipulator," *Electro-Tech.*, 138, Dec., 1960.
 [18] R. S. Mosher, "Handyman to Hardiman," SAE Rep. 670088.
 [19] P. Rabischong, "Robotics for the handicapped," *Proc. IFAC Symp.*, Columbus, OH, May 1982.
 [20] M. W. Spong and M. Vidyasagar, "Robust nonlinear control of robot manipulator," presented at IEEE Conf. on Decision and Control, Dec. 1985.
 [21] M. Vidyasagar, *Nonlinear Systems Analysis*. New York: Prentice-Hall, 1978.



H. Kazerooni (S'84-M'85) received the M.S. degree in mechanical engineering in 1980 from the University of Wisconsin, Madison, and the M.S.M.E. and Sc.D. degrees in mechanical engineering from the Human-Machine Systems Laboratory of the Massachusetts Institute of Technology, Cambridge, in 1982 and 1984, respectively.

From 1984 to 1985 he was with the Laboratory of Manufacturing and Productivity at MIT as a Post-Doctoral Fellow. He is currently an Associate Professor in Mechanical Engineering Department and Control Science Department at the University of Minnesota, Minneapolis, where he holds a McKnight-Land Grant Fellowship.